SINERGI Vol. 23, No. 2, June 2019: 169-174
Accredited **SINTA 2** by KEMENRISTEKDIKTI, Decree No: 10/E/KPT/2019
http://publikasi.mercubuana.ac.id/index.php/sinergi
http://doi.org/10.22441/sinergi.2019.2.011 .

ROTATED RECTANGULAR SLOTS AND MIRRORED INVERSED CANTOR-SETS ON ULTRAWIDEBAND ANTIPODAL VIVALDI ANTENNA

Sabri Alimi, Teguh Prakoso, Munawar Agus Riyadi
Department of Electrical Engineering, Faculty of Engineering, Universitas Diponegoro
Jl. Prof. Soedarto, SH, Semarang, Jawa Tengah 50275, Indonesia
Email: alimi.sabr@gmail.com, teguhprakoso@elektro.undip.ac.id, munawar@elektro.undip.ac.id

Abstract -- *Variants of antipodal Vivaldi antenna (AVA) design suitable for access point working on 0.5 – 6.0 GHz are proposed in this paper. The novel designs were produced by employing three novel techniques to conventional AVA: (i) rotated-slot pattern to shift down the frequency cutoff and enhancing bandwidth, (ii) curve design to miniaturize rotated-slot-inserted antipodal Vivaldi, and (iii) fractal-director (Cantor set) to increase the gain of antipodal Vivaldi. Using FR4 (relative permittivity of 4.4) with an overall dimension of 300 mm x 143 mm x 1.6 mm the antenna designs are able to work at a frequency of 0.472 GHz to higher than 6 GHz with a maximum gain of 11.9 dBi.*

Keywords: *Vivaldi antenna; Rotated rectangular slots; Fractal director; Curve design; Access point*

Received: May 22, 2019 *Revised: June 18, 2019* *Accepted: June 21, 2019*

INTRODUCTION

Gibson proposed tapered slot edge (TSE) antenna or commonly called Vivaldi antenna in 1979 (Gibson, 1979). This kind of antenna offers some advantages such as high direction gain, simple planar structure, and wideband; moreover, conventional Vivaldi antenna has E-plane radiation pattern that is symmetrical with H-plane radiation pattern (Fei et al., 2011). However, this type of antenna needs a quite large dimension (Bang, Lee, & Choi, 2018) that avoids its pervasiveness in applications covering the lower part of UHF. Bandwidth enhancement by lowering cutoff frequency of Vivaldi antenna has been successfully done by inserting corrugation rectangular-slots (Pandey & Meshram, 2015) and employing TSE as corrugation element (Fei et al., 2011) although the low-end frequency shift is still limited. This paper proposes more effective cutoff-frequency decrease by utilizing a pattern of rotated rectangular-slots as corrugation design.

Conventional Vivaldi antenna's flare width cannot less than one wavelength of its lowest frequency of operation (Yngvesson et al., 1989). This antenna can be miniaturized by corrugating its patch curve and ground (Abbosh, 2009). This paper miniaturizes the proposed rotated-slot-corrugated Vivaldi antenna by reducing its length by 10% and then reconfigure the curve profile and rotated-slots' pattern. It is still possible to increase Vivaldi antenna's gain by introducing a parasitic patch as director located at the antenna's aperture. Some published director shapes are elliptical (Nassar & Weller, 2015), rectangular slot (Rahayu & Pohan, 2018; He et al., 2014; Pandey & Meshram, 2015), and asymmetric parasitic patch (Bang et al., 2018). This paper proposes a new fractal-patterned patch as director for Vivaldi antenna. The fractal pattern used in the design is cantor-set.

The goal of the paper is to employ the three techniques to produce antenna for wideband access point working on 0.5 – 6.0 GHz. This frequency range is chosen considering that current and future wireless communications are allocated inside this range. Internet-of-Things devices use the lower part of UHF to achieve long-range communication and preserve their battery lives (Militano et al., 2017). Many applications (Gopal & Kuppusamy, 2017; Tiwari, Keskar, & Shivapakash, 2017) of 5G (ETSI, 2018) in ultra-reliable and low-latency communications work on sub-6 GHz bands. Current wireless communication services employ sub-6 GHz bands, i.e., WiFi, LTE (ETSI, 2011), 3G (ETSI, 2106), and GSM (ETSI, 2017). Wideband access points anticipative to new frequency allocation within 0.5 – 6.0 GHz as well. This condition suggests that antenna working on this frequency range is attractive.

MATERIAL AND METHOD

Material

The antenna designs used FR4 ($\epsilon_r = 4.4$) with thickness of h = 1.6 mm, length of L = 300

mm, and width of W = 143 mm (0.5λ x 0.24λ). At the top and bottom of the PCB, there are copper layers with a thickness of 0.035 mm. Microstrip line for this antenna was calculated for 50 Ohm impedance at 0.5 GHz, with a line length of Lf = 20 mm, and a line width of Wf = 3 mm. CST Microwave Studio simulated antenna design.

Method

A conventional AVA design is illustrated in Fig. 1(a). The antenna curves consist of side, top, and bottom tapers. Bottom taper (see design A in Fig. 2) is constructed from curve governed by the equation:

$$y = 21.49*x^{-0.5541}-1.993 \quad (1)$$

where 1.5306 ≥ x ≥ 71.5. This curve was obtained by manual optimization to achieve good antenna performance, especially on reflection coefficient (S11). From the curve profile, equation (1) was produced by curve fitting facility in Matlab. Taper design positioned on the top (aperture) of Vivaldi antenna (see design E in Fig. 2) was built from a quarter ellipse with major radius (r_{TL}) of 280 mm and minor radius (r_{TW}) of 73.03 mm. Taper design which located on the side of Vivaldi antenna (see design J in Fig. 2) was formed by a half ellipse with major radius (r_{SL}) of 69.97 mm and minor radius (r_{SW}) of 34.98 mm. This design was modified to produce antenna geometries described in Fig. 1(b)-(d). Detail of the modification parameters is illustrated in Fig. 2 and Table 1.

Before conducting all simulations, CST Microwave Studio simulation parameters were set up to be precise and accurate. This simulation was done by simulating Vivaldi antenna design (Fei et al., 2011) and compared the simulation results with antenna performance published (Fei et al., 2011). Good agreement between simulation results and the reference ensures the accuracy and precision of the simulation.

The objective of this paper is to produce high-gain and miniaturized Vivaldi antenna with an operating frequency of 0.5-6.0 GHz. The following three steps have been conducted to obtain the goal.

Table 1. Parameters of Antenna Designs

Parameter	Size (mm) AVA to RSAV	SRSAV
W	143	
L	300	
r_{TW}	73.0306	
r_{TL}	280	259
r_{SW}	34.9847	
r_{SL}	69.9694	62.97246
W_f	3.0612	
L_f	20	18

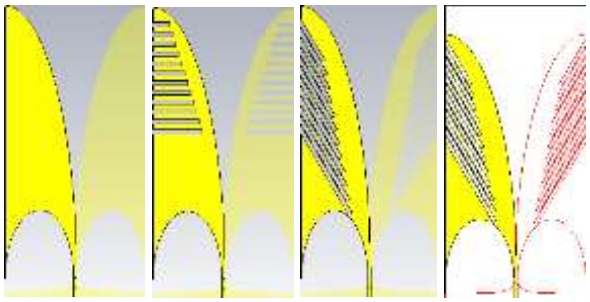

(a) (b) (c) (d)

Figure 1. Antipodal Vivaldi antenna designs: (a) original antipodal Vivaldi antenna (AVA), (b) AVA with corrugation (AVA+Corrugation), (c) AVA with rotated-slot inserted (RSAV), (d) scaled RSAV (SRAV)

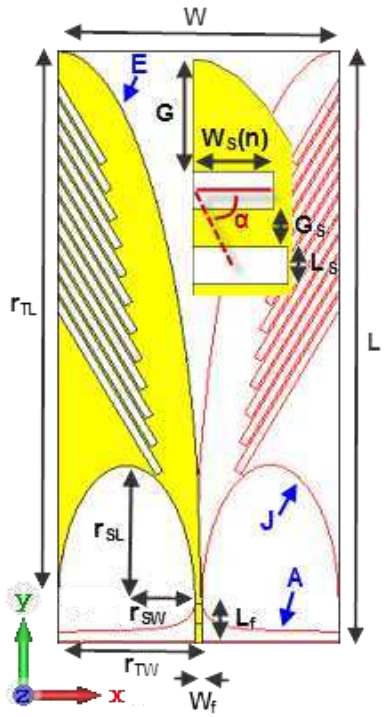

Figure 2. Description of parameter used in Vivaldi antenna designs

The design is decreasing the lower-end of cutoff frequency by rotated-slots insertion

. Twelve rectangular slots were inserted as corrugation to shift down the lower cutoff frequency of conventional AVA; see Fig. 1(b). This pattern is adapted from (Pandey & Meshram, 2015) and called (AVA+Corrugation). The next step was to rotate the slots with the center at the outer side end of the antenna (Fei et al., 2011). Rotated-slot-inserted antipodal Vivaldi (RSAV) as presented in Fig. 1(c) uses a rotation angle of -59°. Description of antenna parameters, including the rotation angle, is illustrated in Fig. 2 and Table 1.

Miniaturizing rotated-slots antipodal Vivaldi with new curve design

Miniaturization was done by reducing the antenna length (L) to be 270 mm, or 90% of its original length. As a consequence, the curve profiles of the antenna were adjusted and the slots were reconfigured as listed in Tabel 1 at column labeled SRSAV (scaled RSAV) and the design is presented in Fig. 1(d). The final value of the slot configuration is listed in Table 2.

Increasing the antenna's gain by incorporating fractal patch as parasitic director

Parasitic patch proposed in this paper is adapted from Cantor-set fractal (Singh, Grewal, & Saxena, 2009); see Fig. 3, combined with a rectangular patch producing final pattern as described in Fig. 4. This parasitic patch is called fractal-director (FD). The values of FD design parameters are F_L = 100 mm and F_W = 30 mm. FD was then inserted to RSAV, as illustrated in Fig. 5(a) whereas FD insertion to SRSAV is presented in Fig. 5(b).

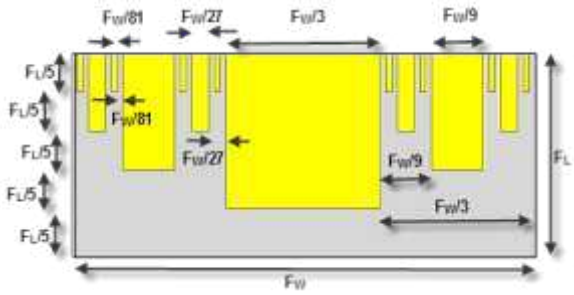

Figure 3. Parasitic patch pattern derived from cantor-set fractal.

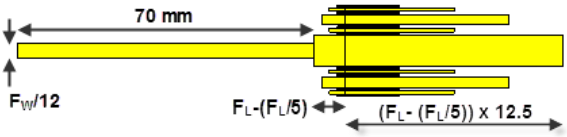

Figure 4. Design of the fractal director (FD)

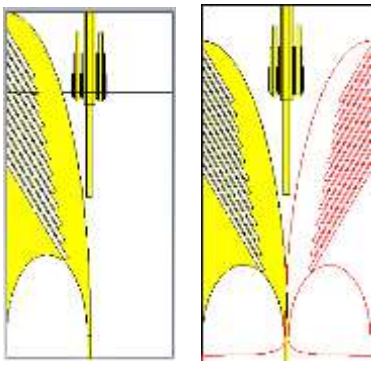

(a) (b)

Figure 5 Patch Fractal Cantor-set implementations in AVA

Table 2. Rectangular slot adjustments for RSAV and SRSAV

Parameter Slot	RSAV	SRSAV
• Rotation angle (degree)	-59	-62
• Distance of 1st slot of the end of antenna L (mm)	14	6.5
• Gap between slots (mm)	6	6.5
• Slot height (mm)	4	3.5
• **Nth Slot width [W_s(n)] (mm) :**		
W_s(1)*	45	55
W_s(2)	50	60
W_s(3)	55	65
W_s(4)	60	70
W_s(5)	65	75
W_s(6)	70	80
W_s(7)	75	85
W_s(8)	80	90
W_s(9)	85	96
W_s(10)	90	102
W_s(11)	95	105
W_s(12)*	100	110

W_s(1): the uppermost slot, and W_s(1): the slot with the lowest position.

RESULTS AND DISCUSSION

Effect of rotated-slots insertion to AVA

Electromagnetic simulations to antenna design in Fig. 1 produce S11 and gain data. Fig. 6 presents simulated S11 for AVA, AVA+Corrugation, RSAV, and SRAV and Fig. 4 compares the maximum gain value of the antenna designs.

Fig. 6 identifies that cutoff frequency (f_c) of AVA is 1.256 GHz, and it also has passband at 0.63-0.92 GHz. Corrugation to the AVA reduce f_c to 970 MHz, and shifts the lowest passband is also shifted to 0.7-0.81 GHz. The existence of stopband between the lowest passbands indicates that resonant point at 0.9 GHz is needed. The new slot pattern insertion is capable to decrease f_c significantly to 487 MHz; it is 767 MHz shift down from AVA's f_c.

The results show that the proposed rotated slots inserted to AVA are very useful in decreasing the lower-edge of AVA's operating frequency. This situation improvement are obtained without altering the antenna's overall size hence the proposed RSAV can be regarded as a very effective method to miniaturize antipodal Vivaldi antenna.

The proposed RSAV also exhibits improvement in gain, as shown in Fig. 7. RSAV's gain is better than AVA, especially for frequency above 1 GHz. Corrugated AVA's gain is higher than RSAV at 1-3 GHz but it is significantly lower at 3-6 GHz. However, the gain of AVA, corrugated AVA, and RSAV are oscillating at a frequency below 1 GHz. At this frequency range, the gain performance of corrugated AVA and RSAV is similar, and AVA's gain is worst among the designs.

Comparison of AVA's, corrugated AVA's, and RSAV's beamwidths are shown in Fig. 8. The beamwidth values go lower as frequency increases beyond 1 GHz. The trend is consistent with the value of gain that increases with frequency. Below 1 GHz the beamwidth values oscillate; when the gain values are low, the beamwidth is large and reach the value of nearly-omnidirectional radiation pattern. The gain, beamwidth, and S11 results prove that RSAV provides significantly better performance than AVA and corrugated AVA. Therefore RSAV becomes the strongest candidate to be miniaturized and gain-enhanced to produce a suitable antenna for wideband access point covering the lower part of the UHF frequency band.

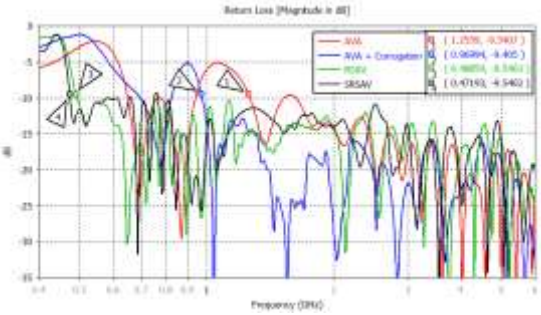

Figure 6. Comparison of simulated reflection coefficient (|S11|) values of original AVA, corrugated AVA, RSAV, and SRAV

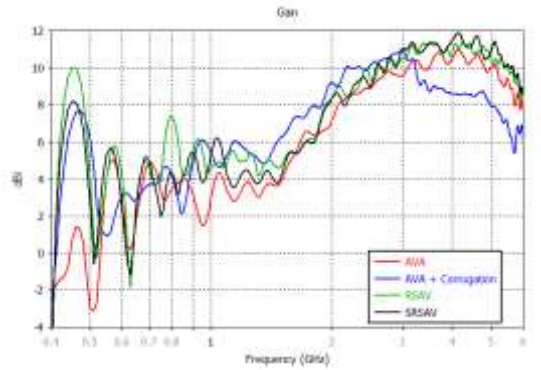

Figure 7. Maximum gain comparison of original AVA, corrugated AVA, RSAV, and SRAV

Effect of curve miniaturization

The length of RSAV can be reduced by changing the Vivaldi curve profile and slot configuration. This miniaturization produces 10% shorter antenna, i.e., 270 mm. Fig. 6 shows that SRSAV's cutoff frequency can be kept similar to RSAV, i.e., 472 MHz. The S11 value of SRSAV is a little bit higher than RSAV at 0.56-0.82 GHz but still below -10 dB. It can be seen that the miniaturized RSAV performance on impedance bandwidth is similar to RSAV.

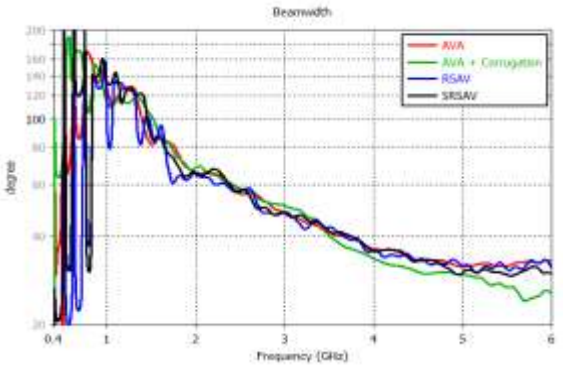

Figure 8. Beamwidth comparison of AVA, corrugated AVA, RSAV, and SRSAV

Gain values of SRSAV are generally better than RSAV for frequency above 1 GHz, see Fig. 7. Similar to other antenna design in Fig. 1, the gain of SRSAV is also oscillating below 1 GHz, but SRSAV has smaller swing than RSAV. Fig. 8 shows that SRSAV's beamwidth is more stable than RSAV's for frequency below 2 GHz. This fact suggests that SRSAV is better than RSAV in term of gain, beamwidth, and physical size.

Effect of fractal-director

Addition of fractal-director (FD) does not change S11 values of RSAV and SRSAV significantly, see Fig. 9. It can be observed that RSAV's and SRSAV's S11 are very similar to their FD counterparts.

The proposed fractal-director design improves SRSAV's gain, especially at frequency larger than 4.7 GHz, see Fig. 10, and Fig. 11. However, the increase in gain value generally less than 0.5 dB. On the contrary, the fractal-director design produces a negative effect on RSAV, see Fig. 10 and Fig. 11. FD can reduce RSAV's gain around 0.5 dB hence it is not suitable to be applied in RSAV.

The maximum gain of the antennas is 11.9 dBi (SRSAV+FD at 4.6 GHz), and SRSAV maximum gain is 11.8 dBi (4.1 GHz), see Fig. 11. It also is interesting to note that all Vivaldi antenna developed and simulated in this paper has gain value above 8 dBi for frequency 2 – 6 GHz, except corrugated AVA only at 2 – 5 GHz. From 1 – 2 GHz, all Vivaldi has gain value above 3 dBi; this suggests that all Vivaldi variants have directive characteristic at 1- 6 GHz. The situation is different for 0.5 – 1.0 GHz. The gain values generally are lower than 3 dBi, at some frequency points are negative, and the value is oscillating over frequency. This value indicates that below 1 GHz the Vivaldi antennas work as small-antenna with radiation-pattern nearly omnidirectional. This indication is supported by beamwidth values as shown in Fig. 12; RSAVs' and SRSAVs'

beamwidth values generally higher than 80 degrees at a frequency below 1.5 GHz.

The function of patch-director mainly to pull the antenna's current distribution to inner-flare side (boresight of the antenna). To attract the present, the distance of the parasitic to the Vivaldi's flare should not be too far. Elliptical (Nasar & Wleer, 2015) and trapezoidal (Bang et al., 2018) patches' sides are quite close to the flare and provide continuous pull to the current in the flare. This is important since gain enhancement is facilitated by current's constructive phase in boresight direction (Nasar & Wleer, 2015). While capable of attracting current, the structure of cantor-director is not that smooth. Hence, phase construction is rather difficult to form in boresight direction.

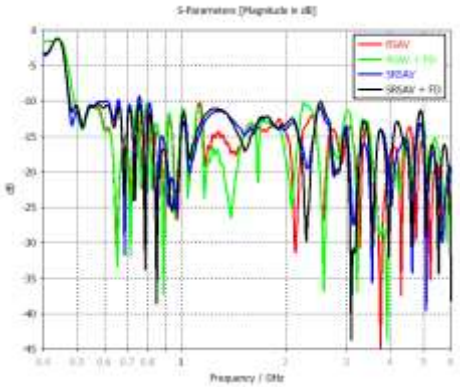

Figure 9. Effect of fractal-director on reflection coefficient of RSAV and SRSAV

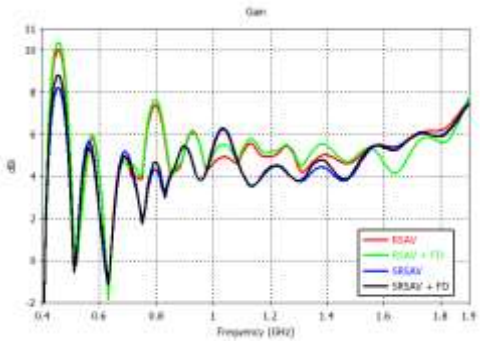

Figure 10. Effect of fractal-director on RSAV's and SRSAV's gain at 0.4 – 1.9 GHz

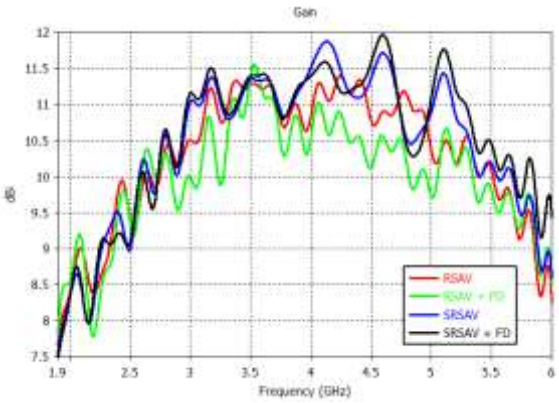

Figure 11. Effect of fractal-director on a gain of RSAVs and SRSAVs at 1.9 – 6.0 GHz

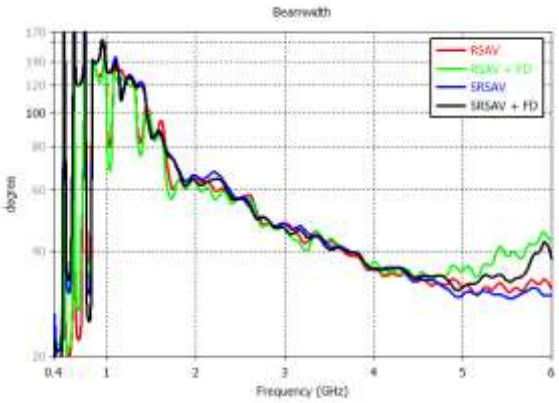

Figure 12. Effect of fractal-director insertion to RSAV and SRSAV

CONCLUSION

The rotated-slot patterns inserted to antipodal Vivaldi as proposed in this paper have been proven capable of reducing the low cutoff frequency from 1.25 GHz to be 0.48 GHz. Ten percent reduction to antenna dimension is facilitated by applying a new curve to the rotated-slot-insertion Vivaldi antenna. The new curve also improves gain. Inclusion of fractal-director (Cantor set) increases the gain of the miniaturized antenna further, around 0.5 dB at a frequency higher than 4.7 GHz. The antennas have directional radiation pattern at frequency 1 – 6 GHz with a maximum gain of 11.9 dBi. From 0.5 to 1 GHz the proposed antennas act as small-antenna with nearly-directional radiation pattern. These suggest that the proposed antenna design can be used for access point working on 0.5 – 6.0 GHz.

REFERENCES

Abbosh, A. (2009). Miniaturized Microstrip-Fed Tapered-Slot Antenna With Ultrawideband Performance. *IEEE Antennas and Wireless Propagation Letters*, *8*, 690–692. https://doi.org/10.1109/LAWP.2009.2025613

Bang, J., Lee, J., & Choi, J. (2018). Design of a Wideband Antipodal Vivaldi Antenna with an Asymmetric Parasitic Patch. *Journal of Electromagnetic Engineering and Science*, *18*(1), 29–34. http://doi.org/10.26886/jees.2018.18.29

ETSI. (2011). LTE Evolved Universal Terrestrial Radio Access (E-UTRA); *Base Station (BS) radio transmission and reception* (3GPP TS 36.104 version 9.13.0 Release 9) (Vol. 0).

ETSI. (2016). Universal Mobile Telelecommunications System ((UMTS); *Base Station (BS) radio transmission and reception (FDD)* (3GPP TS 25.104).

ETSI. (2017). Digital cellular telecommunications system (Phase 2+) (GSM); *GSM/EDGE Radio transmission and reception* (3GPP TS 45.005 version 13.3.0 Release 13).

ETSI. (2018). 5G; NR; *Base Station (BS) Radio Transmission and Reception* (3GPP TS 38.104 version 15.2.0 Release 15).

Fei, P., Jiao, Y.-C., Hu, W., & Zhang, F.-S. (2011). A miniaturized antipodal Vivaldi antenna with improved radiation characteristics. *IEEE Antennas and Wireless Propagation Letters*, *10*, 127–130. https://doi.org/10.1109/LAWP.2011.2112329

Gibson, P. J. (1979). The Vivaldi Aerial. In *9th European Microwave Conference*, *9*, Brighton, UK. (pp.101–105). http://doi.org/10.1109/EUMA.1979.332681

Gopal, B.G. & Kuppusamy, P.G. (2015). A Comparative Study on 4G and 5G Technology for Wireless Applications. *IOSR Journal of Electronics and Communication Engineering (IOSR-JECE)*, *10*(6), 67–72. http://doi.org/10.9790/2834-10636772

He, S. H., Shan, W., Fan, C., Mo, Z. C., Yang, F. H., & Chen, J. H. (2014). An Improved Vivaldi Antenna for Vehicular Wireless Communication Systems. *IEEE Antennas and Wireless Propagation Letters*, *13*, 1505–1508. http://doi.org/10.1109/LAWP.2014.2343215

Militano, L., Orsino, A., Araniti, G., & Antonio, I. (2017). NB-IoT for D2D-Enhanced Content Uploading with Social Trustworthiness in 5G Systems. *Future Internet*, *9*(13), 1–14. https://doi.org/10.3390/fi9030031

Nassar, I. T., & Weller, T. M. (2015). A Novel Method for Improving Antipodal Vivaldi Antenna Performance. *IEEE Transactions on Antennas and Propagation*, *63*(7), 3321-3324. https://doi.org/10.1109/TAP.2015.2429749

Pandey, G. K., & Meshram, M. K. (2015). A Printed High Gain UWB Vivaldi Antenna Design Using Tapered Corrugation and Grating Elements. *International Journal of RF and Microwave Computer-Aided Engineering*, *25*(7), 610–618. https://doi.org/10.1002/mmce.20899

Rahayu, Y. & Pohan, I.A. (2018). Design of Rectangular with Slot Microstrip Antenna for Application LTE 2.1 GHz. *SINERGI*, *22*(2), 127-131. http://doi.org/10.22441/sinergi.2018.2.009

Singh, K., Grewal, V., & Saxena, R. (2009). Fractal Antennas : A Novel Miniaturization Technique for Wireless Communications. *International Journal of Recent Trends in Engineering*, *2*(5), 172–176.

Tiwari, V., Keskar, A., & Shivaprakash, N. (2017). A Reconfigurable IoT Architecture with Energy Efficient Event-Based Data Traffic Reduction Scheme. *International Journal of Online and Biomedical Engineering (IJOE)*, *13*(2), 34-52.

Yngvesson, K. S., Korzeniowski, T. L., Kim, Y. S., Kollberg, E. L., & Johansson, J. F. (1989). The Tapered Slot Antenna—A New Integrated Element for Millimeter-wave Applications. *IEEE Transactions on Microwave Theory and Techniques*, *37*(2), 365–374. https://doi.org/10.1109/22.20062